

# Co-occurrence of resonant activation and noise-enhanced stability in a model of cancer growth in the presence of immune response

Alessandro Fiasconaro and Bernardo Spagnolo

*Dipartimento di Fisica e Tecnologie Relative and CNISM,  
Group of Interdisciplinary Physics\*, Università di Palermo,  
Viale delle Scienze, I-90128 Palermo, Italy*

Anna Ochab–Marcinek and Ewa Gudowska–Nowak

*Marian Smoluchowski Institute of Physics,  
Jagellonian University, Reymonta 4, 30–059 Kraków, Poland†*

(Dated: February 9, 2008)

## Abstract

We investigate a stochastic version of a simple enzymatic reaction which follows the generic Michaelis-Menten kinetics. At sufficiently high concentrations of reacting species, that represent here populations of cells involved in cancerous proliferation and cytotoxic response of the immune system, the overall kinetics can be approximated by a one-dimensional overdamped Langevin equation. The modulating activity of the immune response is here modeled as a dichotomous random process of the relative rate of neoplastic cell destruction. We discuss physical aspects of environmental noises acting in such a system, pointing out the possibility of coexistence of dynamical regimes where noise-enhanced stability and resonant activation phenomena can be observed together. We explain the underlying mechanisms by analyzing the behavior of the variance of first passage times as a function of the noise intensity.

PACS numbers: 82.39.-k, 05.10.-a, 05.40.-a, 82.20.-w

---

\* <http://gip.dft.unipa.it>

†Electronic address: ochab@th.if.uj.edu.pl

## I. INTRODUCTION

The fact which has gained recently considerable attention is that randomly fluctuating systems can behave quite differently from deterministic ones. On the one hand, noise may play a destructive role in natural processes, leading to irregularities or even completely random behavior. On the other hand, random variations may, paradoxically, bring a system to a more ordered state. Phenomena of this kind, e.g. noise-induced transitions, stochastic resonance, noise-enhanced transport or noise-sustained synchronization have been observed in diverse range of systems in physics, chemistry, biology, and medicine [1, 2, 3]. It is becoming apparent that fluctuations and noise are essential ingredients of life processes. Inclusion of stochasticity in mathematical models of biological and biochemical processes is thus necessary for better understanding of mechanisms that govern the biological systems.

The Michaelis-Menten mechanism for enzymatic catalysis is one of the most important mechanisms in biochemistry. The most popular nowadays application of the Michaelis-Menten kinetics is modelling of intracellular biochemical regulation networks, where this sort of kinetics is postulated as one of the standard types of reactions, out of which complex models of cell behavior can be constructed [4]. In a slightly modified form, the Michaelis-Menten reaction scheme turned out to be of practical use in biophysical modelling of radiation-induced damage production and processing. In particular, this reaction scheme has been adapted for the purpose of studying kinetics of double-strand breaks rejoining and formation of simple chromosome exchange aberrations after DNA exposure to ionizing radiation [5]. Similar kinetics has been proposed in saturable repair models of the evolution of radio-biological damage [6].

Another field where the Michaelis-Menten kinetics finds a broad application is population dynamics. Predator-prey models based on that mechanism are very often used in the analysis of population dynamics of bacteria, plankton, plants, or animals [7, 8, 9] in various ecosystems. The cell-mediated immune surveillance against cancer is as well one of the effects which may be described in terms of a "predator-prey" system and be approximated by a saturating, enzymatic-like process whose time evolution equations are similar to the standard Michaelis-Menten kinetics [10, 11, 12]. The population of tumor cells plays here the role of "preys" whereas the immune cells act as "predators". The activity of the predator in a certain territory, or the activity of immune cells in tissue, resemble the mode of action of enzymes or catalysts in a chemical reaction, where the enzymes transform substrates in a continuous manner without destroying themselves. The constant immune cell population is assumed to act in a similar way, binding the tumor cells and subsequently releasing them unable to replicate.

This work is devoted to the study of the Michaelis-Menten kinetics using a stochastic approach. In natural biochemical systems, the enzymatic activity of proteins depends on their configuration, which may be very sensitive to the environment. Random fluctuations of the environmental conditions (e.g. pH, ionic strength) cause changes in enzyme activity. As a result of this, the rate of product formation in the biochemical reaction may deviate significantly from the mean. Because of the exceptionally precise, accurate and efficient nature of biological systems, these deviations may play a crucial role in the functioning of the whole biological system [13]. On the other hand, fluctuations may also play an important role in cancer growth. In the tumor tissue, the growth rate and cytotoxic parameters are influenced by many environmental factors, e.g. the degree of vascularization of tissues, the supply of oxygen, the supply of nutrients, the immunological state of the host, chemical agents, temperature, radiations, gene expression, protein synthesis and antigen shedding from the cell surface, etc. As a result of this complexity, it is unavoidable that in the course of time the parameters of the system undergo random variations which give them a

stochastic character [11, 12, 13, 14, 15, 16].

We will focus here on the interpretation of the Michaelis-Menten reaction as a model for the process of tumor growth. The system is subjected to fluctuating environmental conditions as a whole, and to random variations of the kinetic parameter determining the efficiency of immune response. Modelling the behavior of a tumor, we will be most interested in the possibility of its spontaneous extinction under the influence of random environmental perturbations. In a certain range of values of the parameters describing the immune response intensity and the maximum density of tumor, the model possesses two stable states: the state of extinction, where no tumor cells are present, and the state of stable tumor, where its density does not increase but stays at a certain constant level. Random fluctuations present in the system can induce transitions between those two states. From this point of view, it is interesting to study the mean time of transition from the tumor of a given density (e.g., from the state of a stable tumor) to the state of extinction [17]. We want to find out how the extinction time can be changed by varying the noise parameters, such as intensity or correlation time.

We report the possibility of onset of two noise-induced resonant phenomena in the stochastic Michaelis-Menten reaction under study: the resonant activation and the noise-enhanced stability. In the model of tumor growth, these effects are interpreted as a significant acceleration, or, respectively, deceleration of the spontaneous extinction of tumor. Moreover, we show that the effect of co-occurrence of both mentioned phenomena is possible: A region can be found in the space of noise parameters, where noise-enhanced stability is strongly reduced by resonant activation. An important part of this work is the analysis of the variance of first passage times compared to its mean as a function of the noise intensity, which allowed us to explain in detail the mechanisms underlying the studied phenomena.

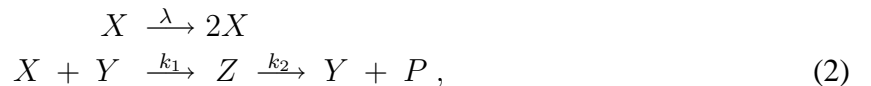
The following section presents the model system used for the analysis of cancer growth kinetics. In the next paragraph we report the results and the appearance of RA and NES phenomena in this model.

## II. THE MODEL SYSTEM

Biochemical reactions are usually described in terms of phenomenological kinetic rates formulated by standard stoichiometric analysis. In such deterministic models, molecular fluctuations can be incorporated by including additional source of stochastic fluxes represented e.g. by an additive white noise  $\xi(t)$ :

$$\frac{dx}{dt} = f(x) - g(x) + \xi(t). \quad (1)$$

The above Langevin equation (further treated in the Ito sense [18]) is based on a continuous description of molecular species: time evolution of an input or output concentrations  $x$  produced at a rate  $f(x)$  and degraded at rate  $g(x)$  defines a deterministic flux of reacting species and can be used when modelling processes involve sufficient concentrations of reacting agents. A Langevin equation with an additive driving noise term is useful to describe molecular fluctuations in terms of infinitesimal changes in an average mesoscopic variable  $x$ , i.e. in concentrations. In that form Eq. (1) will be further postulated to study dynamics of a catalytic reaction. A “free-energy” profile  $U(x) = -\int (f(x) - g(x))dx$  for this reaction is directly derived from the phenomenological Michaelis-Menten scheme for the catalysis accompanying a spontaneous replication of molecules:



where a substrate  $X$  forms first a complex  $Z$  with molecules of the enzyme  $Y$ , before the conversion of  $X$  to a product  $P$  is completed. By assuming that the production of  $X$ -type molecules inhibited by a hyperbolic activation is the slowest process under consideration and by considering a conserved mass of enzymes  $Y + Z = E = \text{const}$ , the resulting kinetics can be recast in the form of the Langevin equation

$$\frac{dx}{dt} = -\frac{dU(x)}{dx} + \xi(t) \quad (3)$$

with the potential  $U(x)$  expressed as

$$U(x) = -\frac{x^2}{2} + \frac{\theta x^3}{3} + \beta x - \beta \ln(x + 1), \quad (4)$$

where  $x$  is the normalized molecular density with respect to the maximum number of molecules, and with the following scaling relations

$$x = \frac{k_1 x}{k_2}, \quad \theta = \frac{k_2}{k_1}, \quad \beta = \frac{k_1 E}{\lambda}, \quad t = \lambda t. \quad (5)$$

Note that the very same approach aimed to reduce the dimension of the chemical master equation by employing so called quasi-steady-state approximation [19, 20] (applicable when a subset of species is at steady state at the time scale of interest) is broadly used in description of stochastic chemical kinetics. In particular, for the enzymatic reactions described by the Michaelis-Menten scheme, the quasi-steady-state approximation assumes much larger concentration of substrates  $X$  than the enzyme concentration  $E$ . This, by considering the steady state constraint  $dZ/dt = 0$ , becomes equivalent to assuming that the propensity function for the decay of  $X$  molecules is given, in rescaled variables (Eq. (5)), by  $-\beta x/(1 + x)$ . The resulting potential profile Eq. (4) has at most three extremes representing deterministic stationary states of the system (see Fig. 1):

$$x_1 = 0, \quad (6)$$

$$x_2 = \frac{1 - \theta + \sqrt{(1 + \theta)^2 - 4\beta\theta}}{2\theta}, \quad (7)$$

$$x_3 = \frac{1 - \theta - \sqrt{(1 + \theta)^2 - 4\beta\theta}}{2\theta}. \quad (8)$$

The essential feature captured by the model is, for a constant parameter  $\theta$ , the  $\beta$ -dependent bistability. In the above form and by assuming time dependent random variations of the parameter  $\beta$ , the model has been used to describe an effect of cell-mediated immune surveillance against the cancer [12] or, alternatively, to analyze the stochastic amplification and signaling in futile enzymatic cycles [20]. The immunological defense mechanisms involve cell-mediated responses that consist in each case of recognition processes of the cancer followed by their destruction as proliferating cells. Most of tumoral cells bear antigens which are recognized as strange by the immune system. A response against these antigens may be mediated either by immune cells such as T-lymphocytes or other cells, not directly related to the immune system (like macrophages or natural killer cells). The process of damage to tumor proceeds via infiltration of the latter by the specialized cells, which subsequently develop a cytotoxic activity against the cancer cell-population. The series of cytotoxic reactions between the cytotoxic cells and the tumor tissue have been documented to be well approximated [12] by a saturating, enzymatic-like process whose time evolution equations are similar to the standard Michaelis-Menten kinetics. The variability of kinetic parameters defining this process naturally affects the extinction of the tumor [11, 12] and points to the

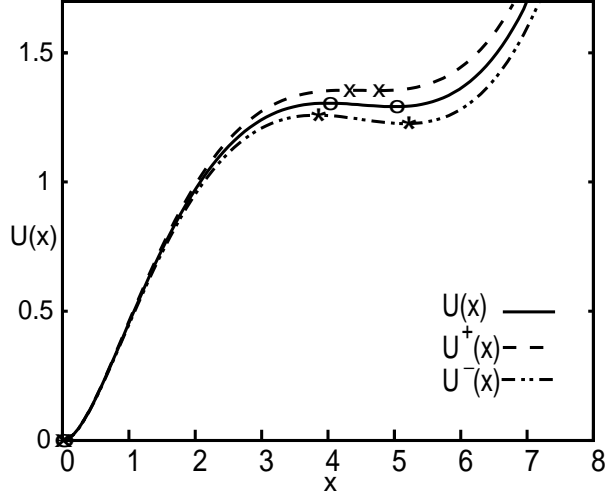


FIG. 1: The Michaelis-Menten potential with parameters:  $\beta = 3, \theta = 0.1, \Delta = 0.02$ . Labels: “o”: extremes of  $U(x): x = 0, 4, 5$ ; “x”: extremes of  $U^+(x): x = 0, 4.28, 4.72$ ; “\*”: extremes of  $U^-(x): x = 0, 3.83, 5.17$ .

special role played by the parameters  $\theta$  and  $\beta$ , as described in [11]. The T-helper lymphocytes and macrophages, can secrete cytokines in response to stimuli. The functions that cytokines induce can both “turn on” and “turn off” particular immune responses [21]. The immune modulating activities of cytokines are a result of their influence on gene expression, protein synthesis and antigen shedding from the cell surface [14, 15, 16]. This “on-off” modulating regulatory role of the cytokines is here modelled through a dichotomous random variation of the parameter  $\beta$ , by taking into account the natural random fluctuations always present in biological complex systems.

The mean escape time has been intensively studied in order to characterize the lifetime of metastable states of static and fluctuating potentials with different initial conditions [22, 23, 24, 25, 26, 27, 28, 29, 30, 31, 32, 33, 34]. These studies show that the mean escape time has different non-monotonic behaviors as a function of both the thermal noise intensity and the mean frequency of potential fluctuations. These behaviors are a signature of two noise-induced effects, namely the resonant activation (RA) [22, 23, 24, 25, 26, 27, 28, 29] and the noise enhanced stability (NES) [30, 31, 32, 33, 34]. NES, a phenomenon described theoretically and observed experimentally and numerically in different physical systems, stabilizes a fluctuating metastable state in such a way that the system remains in this state for a longer time than in the absence of white noise. On the other hand, due to the RA phenomenon, the mean escape time from the metastable state across the fluctuating barrier may exhibit non-monotonic dependence on the characteristic time scale of these fluctuations.

In the model system investigated here we consider a chemical Langevin equation with two independent sources of external fluctuations represented by an additive driving noise term and a dichotomous Markovian noise multiplying the  $\beta$  parameter (see Eq. (5)). The latter is responsible for regulatory inhibition of the population growth and represents the modulating stochastic activity of the cytokines on the immune system [14, 15, 16]. This process can change the relative stability of metastable states and, in consequence, reverse the direction of the kinetic process at hand. It should be emphasized that the above mentioned phenomena of RA and NES act counter to each other in the cancer growth dynamics: the NES effect increases in an unavoidable way the average lifetime of the metastable state (associated to a fixed-size tumor state), while the RA

phenomenon minimizes this lifetime. Therefore, the purpose of this work is to find the optimal range of parameters in which the positive role of resonant activation phenomenon, with respect to the cancer extinction, prevails over the negative role of NES, which enhance the stability of the tumoral state.

We adhere to the model of an overdamped Brownian particle moving in a potential field between absorbing and reflecting boundaries in the presence of noise which modulates the barrier height. The evolution of a state variable  $x(t)$  is described in terms of the Langevin equation

$$\frac{dx}{dt} = -\frac{dV(x, t)}{dx} + \sigma\xi(t),$$

$$V(x, t) = U(x) + G(x)\eta(t). \quad (9)$$

Here  $\xi(t)$  is a Gaussian process with zero mean and correlation function  $\langle \xi(t)\xi(t') \rangle = \delta(t - t')$ , and  $\sigma$  is the noise intensity. The potential  $V(x, t)$  is the sum of two terms: the fixed potential  $U(x)$  and the randomly switching term  $G(x)\eta(t)$ , where  $\eta(t)$  stands for a Markovian dichotomous noise switching between two levels  $\{\Delta^+, \Delta^-\}$  with correlation time  $\tau$  and mean frequency  $\nu = 1/(2\tau)$ . This means that its autocorrelation function is

$$\langle (\eta(t) - \langle \eta \rangle)(\eta(t') - \langle \eta \rangle) \rangle = \frac{(\Delta^+ - \Delta^-)^2}{4} e^{-|t-t'|/\tau}.$$

Both noises are assumed to be statistically independent, *i.e.*  $\langle \xi(t)\eta(s) \rangle = 0$ . The potential  $V(x, t)$  therefore flips at random time between two configurations

$$U^\pm(x) = U(x) + G(x)\Delta^\pm. \quad (10)$$

Based on Eq. (9), we can write a set of Fokker-Planck equations which describe the evolution of probability density of finding the state variable in a “position”  $x$  at time  $t$ :

$$\begin{aligned} \partial_t p(x, \Delta^\pm, t) &= \partial_x \left[ \frac{dU^\pm(x)}{dx} + \frac{1}{2}\sigma^2 \partial_x \right] p(x, \Delta^\pm, t) \\ &\quad - \frac{1}{2\tau} p(x, \Delta^\pm, t) + \frac{1}{2\tau} p(x, \Delta^\mp, t). \end{aligned} \quad (11)$$

In the above equations time has dimension of  $[length]^2/energy$ , due to a friction constant that has been “absorbed” in a time variable. With the initial condition

$$p(U^\pm, x_s, t)|_{t=0} = \frac{1}{2}\delta(x - x_s), \quad (12)$$

from Eqs. (11) we get the equations for the mean first passage times (MFPTs):

$$\begin{aligned} -1 &= -\frac{T^+(x)}{\tau} + \frac{T^-(x)}{\tau} - 2\frac{dU^+(x)}{dx} \frac{dT^+(x)}{dx} + \sigma^2 \frac{d^2 T^+(x)}{dx^2} \\ -1 &= \frac{T^+(x)}{\tau} - \frac{T^-(x)}{\tau} - 2\frac{dU^-(x)}{dx} \frac{dT^-(x)}{dx} + \sigma^2 \frac{d^2 T^-(x)}{dx^2}, \end{aligned} \quad (13)$$

where  $T^+(x)$  and  $T^-(x)$  denote MFPT for  $U^+(x)$  and  $U^-(x)$ , respectively. The overall MFPT for the system reads

$$T(x) = T^+(x) + T^-(x), \quad (14)$$

with boundary conditions

$$\begin{aligned}\frac{dT^\pm(x)}{dx}\bigg|_{x=a} &= 0, \\ T^\pm(x)\bigg|_{x=b} &= 0,\end{aligned}\tag{15}$$

which correspond to a reflecting boundary at  $x = a$  and an absorbing boundary at  $x = b$ . As in the usual physical picture of resonant activation phenomenon [22] we expect that, for the frequency of potential switching tending to zero (long correlation time of the dichotomous noise  $\eta(t)$ ), MFPT for the switching barrier will be a mean value of MFPTs for both configurations

$$\lim_{\tau \rightarrow \infty} T(U^+, U^-, \tau) = \frac{1}{2} (T^+ + T^-), \tag{16}$$

where the  $T^+$  and  $T^-$  are obtained for fixed potentials with  $U^+$  and  $U^-$  respectively (Eq. (10)). For the switching frequency tending to infinity (short correlation time), the system will “experience” a mean barrier

$$\lim_{\tau \rightarrow 0} T(U^+, U^-, \tau) = T\left(\frac{U^+}{2} + \frac{U^-}{2}\right). \tag{17}$$

Although the solution of the system (13) is usually unique [22], a closed, “ready to use” analytical formula for MFPT can be obtained only for the simplest cases of potentials. More complex cases require either use of approximation schemes [23, 25, 26], perturbative approach [24], or direct numerical evaluation methods [28].

The kinetics of our biological system is described by the equation

$$\frac{dx}{dt} = (1 - \theta x)x - \beta \frac{x}{x + 1}, \tag{18}$$

where  $x(t)$  is the concentration of the cancer cells. The profile of the corresponding quasi-potential (Eq. (4)) presents a double well with one of the minima at  $x = 0$ . The region for  $x > 0$  can show either a monotonic behavior or a local minimum, depending on the values of parameters  $\theta$  and  $\beta$ . In the present investigation we used only parameters able to give a local minimum of the Michaelis-Menten potential for  $x > 0$ :  $\theta = 0.1$  and  $\beta = 3$  (see Fig. 1). For  $x \rightarrow \infty$  the potential shows a strong cubic repulsion. Taking into account a random fluctuating environment (temperature, chemical agents, radiation, etc.), we joined an additive noise term  $\sigma\xi(t)$  to the Eq. (18). In order to describe realistic fluctuations in immune response [14, 15, 16], we added a dichotomous Markovian noise  $\eta(t)$ , of amplitude  $\Delta$  and mean correlation time  $\tau$ , to the  $\beta$  parameter. A contribution of this kind implies that the effective potential switches between two conformational states  $U^\pm(x)$ . Taking into account all the noise contributions, we obtain the stochastic Michaelis-Menten potential

$$U^\pm(x) = -\frac{x^2}{2} + \frac{\theta x^3}{3} + (\beta \pm \Delta)(x - \ln(x + 1)), \tag{19}$$

and the Langevin equations for the system

$$\begin{aligned}\dot{x} &= -\frac{dU^\pm(x)}{dx} + \sigma\xi(t) \\ &= x(1 - \theta x) - (\beta \pm \Delta)\frac{x}{x + 1} + \sigma\xi(t).\end{aligned}\tag{20}$$

The process of population growth and decay can be described as a motion of a fictitious particle in the switching potential between two configurations  $U^+(x)$  and  $U^-(x)$ . The presence of noise

modulates the height of the barrier dividing two stable states of the population. Transitions from one state to the other (here: from a fixed-size tumor to a cancer-free state or *vice versa*) are induced by an additive thermal-like noise [35]. For negligible additive noise and small concentration of tumor cells, this model resembles a standard Verhulst equation with perturbing multiplicative dichotomous noise, which exhibits a complex scenario of noise-induced transitions, observable in a pattern of the stationary probability density [1]. Here, we will address kinetic properties of this model by studying the mean first passage time (14) between high and low population states in the system. We will study how the two different sources of noise as well as the position of the starting point  $x_{\text{in}}$  influence the mean first passage time. We put the absorbing boundary at  $x = 0$  and the reflecting one at  $x = \infty$ . The event of passing through the absorbing boundary is equivalent to a total extinction of cancer.

### III. RESULTS

In order to obtain the MFPT for various starting points  $x_{\text{in}}$ , we performed a series of Monte-Carlo simulations of the stochastic process (20) with an absorbing boundary at  $x = 0$ , reflecting boundary at  $x = +\infty$  and the values of parameters:  $\beta = 3$ ,  $\theta = 0.1$ ,  $\Delta = \pm 0.02$ . The statistics for each MFPT has been taken from  $10^3$  simulation runs, except for the results shown in Figs. 6 - 8 where  $10^4$  simulation runs were performed. The results confirm the existence of resonant activation and noise-enhanced stability phenomena in the studied system. Moreover, we have shown that in a certain range of parameters both effects can occur together.

#### A. Resonant activation

The resonant activation phenomenon occurs when, at a given intensity  $\sigma$  of the additive noise, there exists a certain mean frequency  $\nu_{\text{min}}$  (and correspondingly a correlation time  $\tau_{\text{min}}$ ) of the multiplicative noise, at which the mean first passage time is shortest. The resonant activation effect minimizes the average lifetime of a population in the metastable state. Let us assume that the Brownian particle is behind the potential barrier, in a neighborhood of the metastable state. When the barrier fluctuations are very fast ( $\tau$  small), the particle “can never adjust” to the instantaneous slope of the potential. Instead, it “perceives” a slope which is an average of the higher and lower configurations. The MFPT will tend to a constant value corresponding to the average static potential. If the barrier fluctuations are slower than the actual escape rate ( $\tau$  large), the particle will escape before any barrier flip occurs. Therefore, the mean first passage time also tends to a constant, which now will be an average of the escape times for the higher and lower configurations of the potential. At the intermediate values of  $\tau$ , the escape rate is an average of the escape rates for the higher and lower configurations of the potential [23, 27]. In other words, MFPT is the inverse of the mean escape rate, and, because of its approximately exponential dependence on the ratio between the height of the barrier and the noise intensity, its value is lower than both above mentioned asymptotic mean first passage times [27].

We compared the effect of resonant activation in the Michaelis-Menten potential for trajectories starting from various points: the neighborhood of the right minimum (bottom of the potential well), the neighborhood of the barrier top, and two points on the left slope of the barrier. In Fig. 2 we plot the MFPT as a function of the correlation time  $\tau$ . The RA effect is well visible for trajectories starting from behind the potential barrier and even for those starting from its top. If the trajectories start from the outer slope of the barrier, only a small fraction of them can surmount it and be



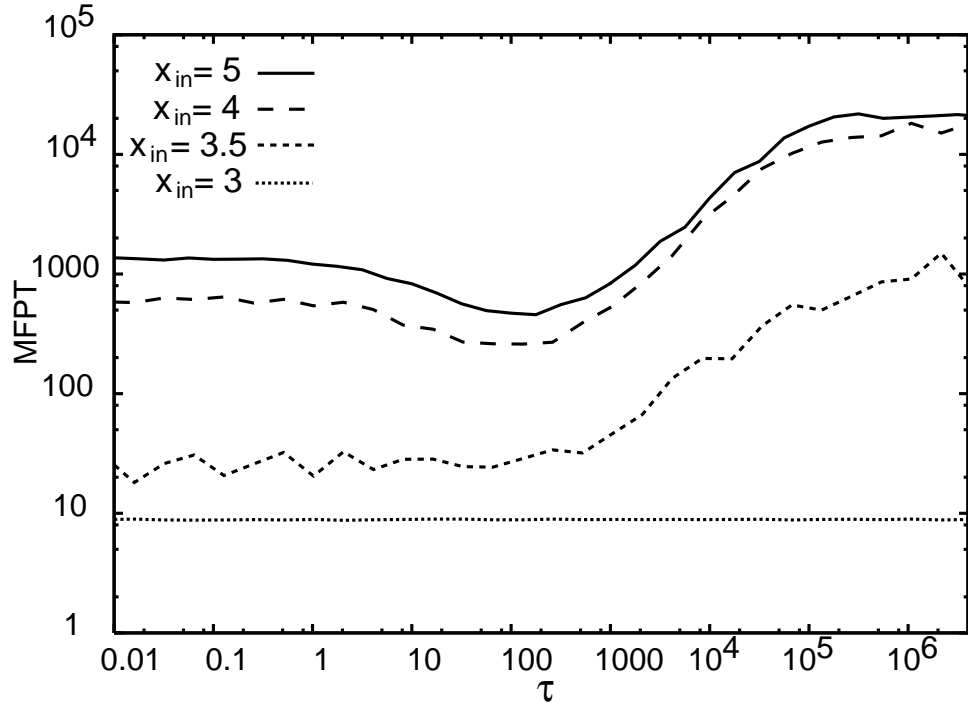


FIG. 2: MFPT as a function of correlation time  $\tau$  of the dichotomous noise, for various starting points  $x_{\text{in}}$  in the Michaelis-Menten potential. The RA effect is well visible for initial positions near the metastable state and near the maximum of the potential. Initial positions:  $x_{\text{in}} = 5$  (in the neighborhood of the right minimum),  $x_{\text{in}} = 4$  (in the neighborhood of the maximum),  $x_{\text{in}} = 3.5$  (left slope),  $x_{\text{in}} = 3$  (left slope). The parameter values are:  $\beta = 3$ ,  $\theta = 0.1$ ,  $\Delta = 0.02$ , and  $\sigma = 0.1$ .

trapped in the potential well, which would produce the effect of resonant activation. Most of them rather run down the slope and approach the absorbing barrier without having been trapped. This is the obvious reason why the MFPTs for such initial points are shorter and their graphs less accurate: The numerous contributions from the trajectories which were not trapped are responsible for the shortening of MFPT. On the other hand, only a small number of contributions from trapped trajectories are responsible for the resonant activation effect. Since the trapping events are very rare for  $x_{\text{in}}$  lying on the outer slope, the statistics taken from a sample of 1000 simulation runs turns out to be too small to produce a clear image of RA.

## B. Noise-enhanced stability

The noise-enhanced stability effect occurs when, at a given mean frequency  $\nu$  of the multiplicative noise, there exists a certain intensity  $\sigma_{\text{max}}$  of the additive noise, at which the mean first passage time is longest. Differently from RA, the NES effect maximizes the average lifetime of the population in a metastable state as a function of the noise intensity. The nonmonotonic behavior of the mean escape time as a function of the additive noise intensity  $\sigma$  depends on the potential profile parameters, on the parameters of the multiplicative dichotomous noise and also on the initial position of the Brownian particle [31, 32, 34]. Noise enhances the stability of the metastable state with different peculiarities related to different dynamical regimes: the average lifetime can

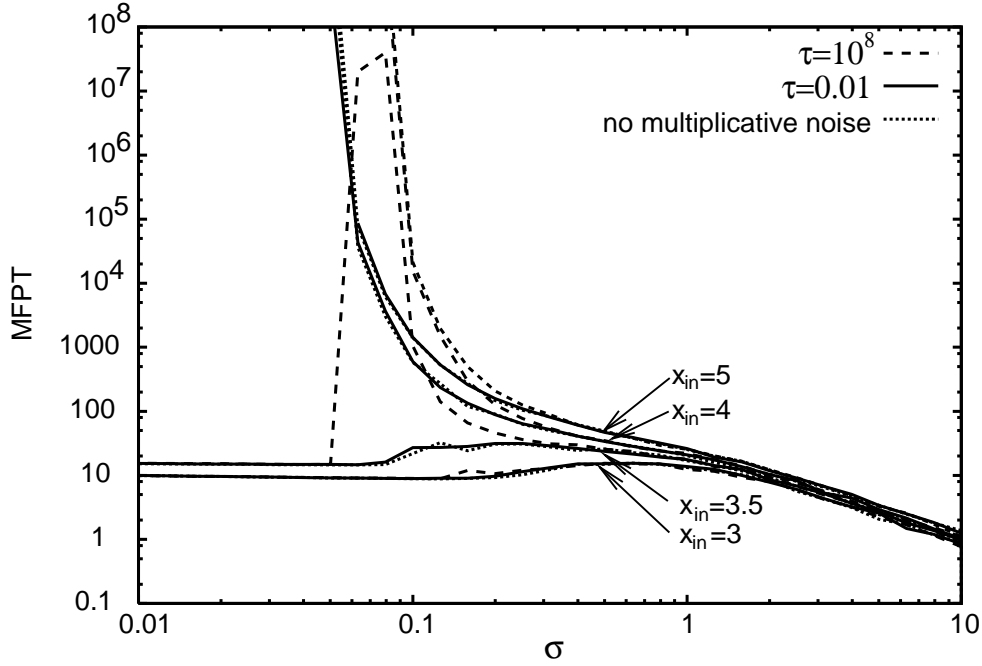


FIG. 3: MFPT as a function of the noise intensity  $\sigma$ . Influence of the multiplicative dichotomous noise on the NES effect for the same initial positions as in Fig. 2 and two values of correlation time of the dichotomous noise, namely:  $\tau = 0.01$  (solid line) and  $\tau = 10^8$  (dashed line). All the other parameters are the same of Fig. 2. The MFPTs in the absence of multiplicative noise (dot lines), that is for an average fixed barrier, are compared with those calculated at very low correlation time  $\tau$  (solid line).

greatly increase when the noise intensity is very low with respect to the height of the barrier and the initial positions of the Brownian particles are in the “divergent” dynamical regime [34].

If the particle starts from initial positions within the potential well, at small values of  $\sigma$  it will rather stay trapped in the well than escape from it, according to the Kramers formula. The mean escape time will then tend to infinity for  $\sigma \rightarrow 0$ . If the particle starts from outside the well, at small  $\sigma$  it will at once run down the slope and its mean escape time will tend to the escape time of a deterministic particle. At high noise intensities, the mean escape time decreases monotonically, regardless of initial positions. At intermediate noise intensities, a particle starting from the outer slope may sometimes be trapped into the well. Such events, although rare, can significantly increase the mean escape time because a trapped particle stays then in the well for a relatively long time.

In Fig. 3 we show how the dichotomous barrier switching influences the NES effect. If the mean switching frequency  $\nu$  is large, then the MFPT behaves as the mean first passage time for an average barrier, so the NES effect looks like in a potential with no multiplicative noise ( $\Delta = 0$ ). When, in turn, the mean switching frequency  $\nu$  is very small, then the MFPT is an average of the mean first passage times for the higher and lower position of the switching potential (see Fig. 4). Here the NES effect can sometimes differ considerably from the same effect in the static potential, even if the amplitude of the dichotomous noise  $\Delta$  is very small with respect to the value of the  $\beta$  parameter.

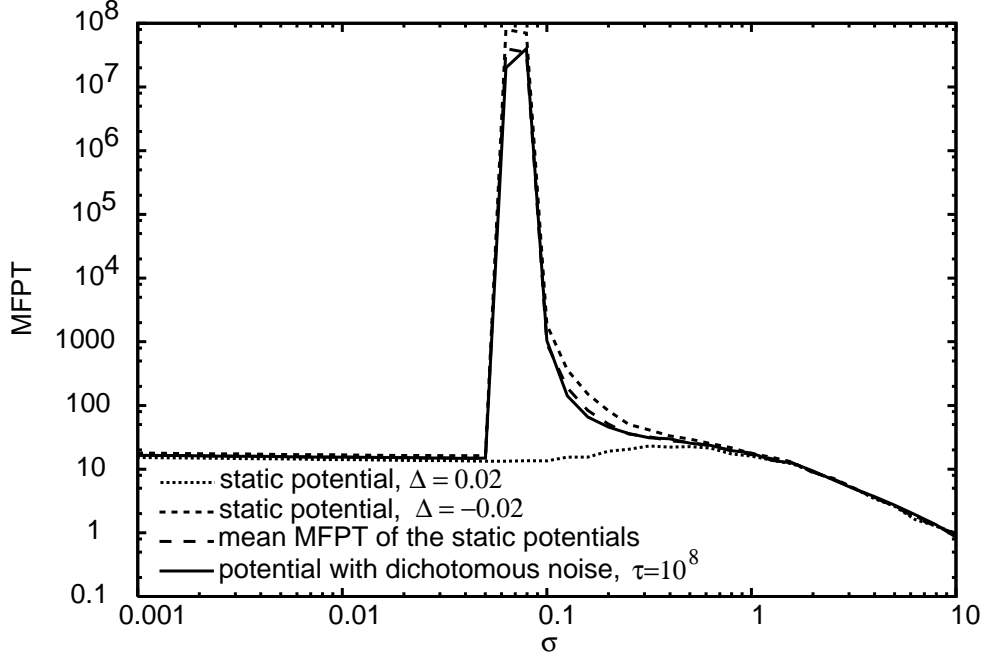


FIG. 4: MFPT for the higher (dot line) and lower (short dashed line) position of the switching potential and their mean, as a function of the noise intensity  $\sigma$ . Although  $\Delta$  is small, the NES effect in a static potential with  $\beta + \Delta$  looks quite different from that obtained with  $\beta - \Delta$ . The mean MFPT of the static potentials (long dashed line) is compared with the MFPT calculated at very small switching frequency of the dichotomous noise. The initial position is  $x_{\text{in}} = 3.5$ , and all the other parameter values are the same as in Fig. 2.

### C. Noise-enhanced stability vs. resonant activation

In Figs. 5 and 6 we present the combined view of RA and NES effects. We notice that RA is better visible when the additive noise is weak compared to the height of the barrier.

If the potential barrier is high enough or the additive noise is weak enough, the mean first passage time in a static potential can be approximated by the inverse of the Kramers escape rate, which increases exponentially with  $\Delta U(x)/\sigma^2$ , where  $\Delta U(x)$  is the height of the barrier. Such an exponential dependence guarantees the existence of a minimum of  $\text{MFPT}(\tau)$ . Its value at intermediate  $\tau$  is lower than both asymptotic mean first passage times, for very large or very small  $\tau$ . Specifically the MFPT at very low mean switching frequency  $T_{\tau \rightarrow \infty} (= \frac{1}{2}[T^+ + T^-])$ , will be higher than the MFPT at the high frequency limit  $T_{\tau \rightarrow 0} (= T(\frac{U^+}{2} + \frac{U^-}{2}))$ . In the middle frequency regime the effective escape rate over the fluctuating barrier is the average of the escape rates ( $\frac{1}{2}(K_+ + K_-)$ , where  $K_+ = 1/T^+$  and  $K_- = 1/T^-$ , with  $K_+ \gg K_-$ , and because of the exponential dependence, the MFPT in this intermediate frequency regime will be smaller than  $T_{\tau \rightarrow 0}$ . The resonant activation phenomenon therefore will manifestly occur if  $\sigma \ll \Delta(U_{\text{max}}^+ - U_{\text{max}}^-)$ , where  $\Delta(U_{\text{max}}^+ - U_{\text{max}}^-)$  is the difference in height between the higher and lower position of the barrier at the maximum of the potential well [27]. In the case of our potential, that difference is of order  $10^{-1}$ , so the resonant activation can be observed for  $\sigma < 10^{-1}$  as we can see from Fig. 5.

To show better the RA phenomenon in the parameter region of NES, we must choose an appropriate initial condition  $x_{\text{in}}$ . In order to obtain a well-visible RA (a large enough number of

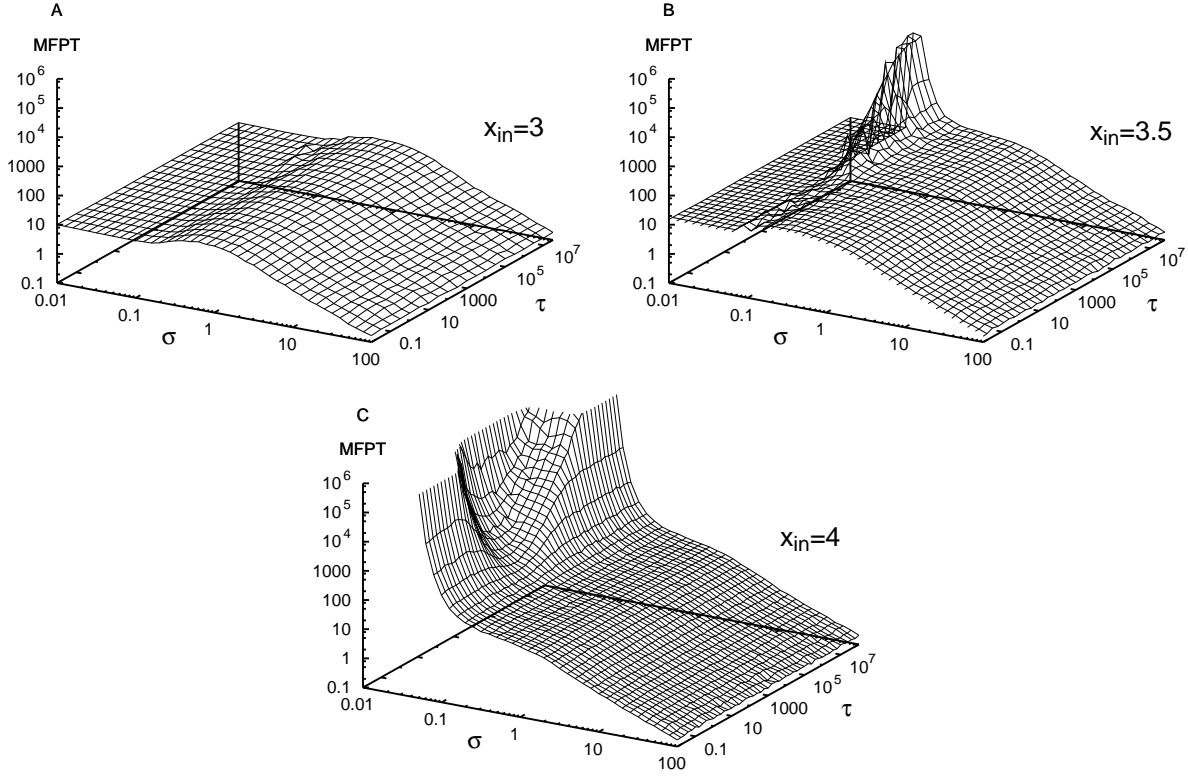


FIG. 5: NES vs RA: three-dimensional plot of MFPT as a function of noise intensity  $\sigma$  of the additive noise and correlation time  $\tau$  of the dichotomous noise. The initial positions of the Brownian particle and all the other parameter values are the same as in Fig. 2.

trajectories trapped in the potential well) we have to choose the initial position sufficiently close to the top of  $U^-(x)$ . We report in the following Fig. 6 the co-occurrence of resonant activation and noise-enhanced stability at  $x_{\text{in}} = 3.6$ . Since both effects act here in an opposite way, there exists a regime of  $\sigma$  and  $\tau$  parameters where noise-enhanced stability is strongly reduced by resonant activation.

The above considerations are valid not only for trajectories starting from inside the potential well, but also for arbitrary initial positions in the potential, if only the particle has a chance to be trapped behind the potential barrier for some time. If the additive noise intensity is very large, a particle starting from the outer slope of the barrier does not “feel” the barrier at all. If, in turn, the additive noise is very weak, the particle slides down the slope in an almost deterministic way. But at intermediate values of  $\sigma$ , the particle can (in some realizations) be trapped behind the barrier and, in case of such a rare event, its escape time changes non-monotonically as a function of  $\tau$ , in a way described in subsection III A. This effect of coexistence of noise-enhanced stability and resonant activation effects can be observed in Fig. 6. In Fig. 7 we report the cross-sections of Fig. 2, in the region of coexistence of RA and NES, for five values of the additive noise intensity  $\sigma$ , namely:  $\sigma = 0.050, 0.063, 0.079, 0.100, 0.126$ . The effect of the RA overlapping the NES is well visible. It is clear that for noise intensity values greater than  $\sigma \approx 0.1$ , the nonmonotonic behavior typical of RA effect disappears.

In Fig. 8 we present the graphs of MFPT vs. additive noise intensity  $\sigma$  together with the standard deviation of  $N = 10^4$  first passage times, at  $\tau = 10^5$  (slow switching) and  $\tau = 10^0$  (fast

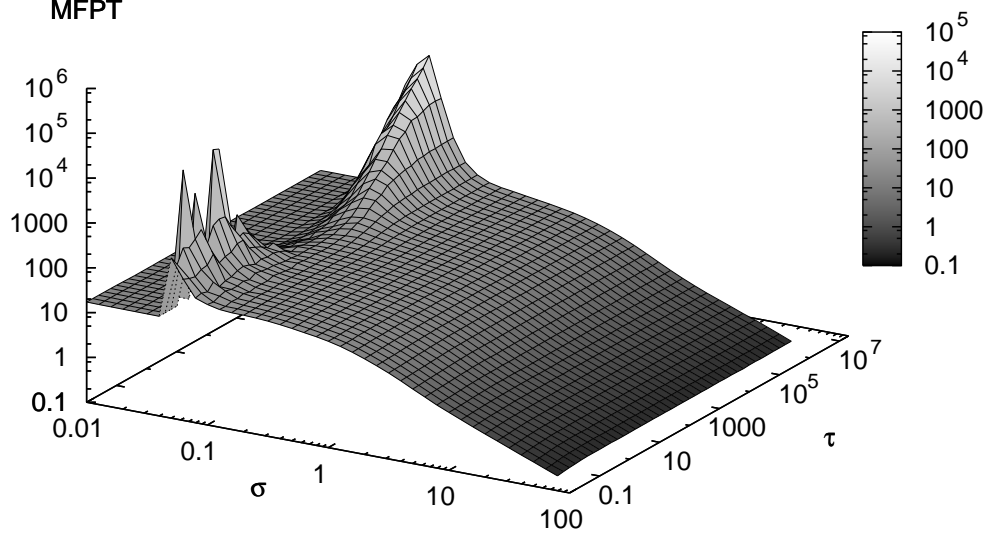


FIG. 6: The coexistence of NES and RA phenomena in a three-dimensional plot of MFPT as a function of noise intensity  $\sigma$  and correlation time  $\tau$ . The initial position of the Brownian particle is  $x_{\text{in}} = 3.6$ . Number of simulation runs  $N = 10^4$ . All the other parameter values are the same as in Fig. 2.

switching). The initial position has been set up to  $x_{\text{in}} = 3.6$ . At large intensities of the additive noise the standard deviation is equal to MFPT, which indicates the purely Arrhenius behavior of the system kinetics [36]. This can be explained in the following way: if the additive noise is strong enough, the Brownian particle does not "feel" the random changes in the height of potential barrier and its motion becomes diffusive. In the region of NES, the system's behavior begins to diverge from the Arrhenius model and typically, the standard deviation is much higher than the mean of first passage times. On the other hand, at small intensities of the additive noise, the standard deviation is much lower than the mean. In the range of  $\sigma$  where the NES occurs, the possible trajectories can be roughly divided into the "short" ones, which were not trapped but ran down to the absorbing boundary at  $x = 0$ , and the "long" ones, which were trapped behind the potential barrier for a long time. In a sample of registered  $N = 10^4$  first passage times, we observe a large number of "short" times of order of 10, whose standard deviation is of order of 1, and a small number of "long" times of order of  $10^5$  (at  $\tau = 10^5$ ) or  $10^7$  (at  $\tau = 10^0$ ) whose standard deviation is of order of  $10^5$  (at  $\tau = 10^5$ ) or, respectively,  $10^7$  (at  $\tau = 10^0$ ). The contribution of "long" trajectories to the overall standard deviation makes it very large. However, the weaker the additive noise is, the smaller is the number of trapped trajectories and their contribution to the standard deviation. In the region of small  $\sigma$ , where the standard deviation is smaller than MFPT, no trapped trajectories were recorded. It suggests that the region is dominated by an almost deterministic kinetics with contributions from the stochastic diffusion visible mostly in a flat part of the potential well close to  $x = 0$ .

It should be noted, however, that the behavior of MFPT shown in Fig. 8a, at the fast switching of the potential profile ( $\tau = 1$ ) and with the initial position  $x_{\text{in}} = 3.6$ , corresponds, in the limit

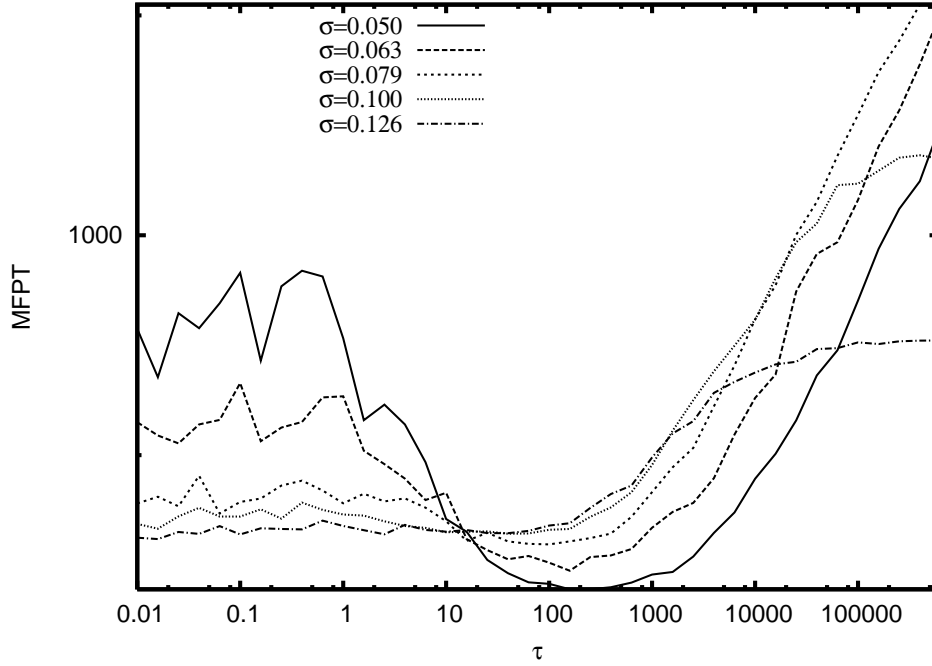


FIG. 7: Cross-sections of Fig. 6 for six values of the noise intensity  $\sigma$ , in the region of coexistence of RA and NES. The effect of resonant activation overlapping the noise-enhanced stability is well visible. The initial point is  $x_{\text{in}} = 3.6$ . Number of simulation runs  $N = 10^4$ . All the other parameter values are the same as in Fig. 2.

of  $\tau \rightarrow 0$ , to a Brownian particle moving in a fixed potential (the average potential profile  $U(x)$  of Fig. 1) starting from an initial unstable state and in a divergent dynamical regime with regards to the MFPT (see Ref. [34] for a detailed discussion on this point). In this regime both the MFPT and its standard deviation (SD) diverge for  $\sigma \rightarrow 0$ . Because of the finiteness of the ensemble of realizations and of the observation time considered in our numerical experiments we don't observe the divergence of MFPT and its SD, and for  $\sigma \rightarrow 0$  the deterministic escape time is obtained. While the behavior shown in Fig. 8b corresponds to the "real" nonmonotonic behavior of MFPT and its SD as a function of the noise intensity  $\sigma$ . These different dynamical regimes experienced by the Brownian particle explain the two behaviors of Fig. 8. As a consequence we expect very large error bars just in the maximum value of MFPT (Fig. 8a), and decreasing error bars by increasing noise intensity values. This error bar behavior should be considered as a signature of the divergent dynamical regime in the NES effect.

#### IV. CONCLUSIONS

We studied a Langevin equation derived from the phenomenological Michaelis-Menten scheme for catalysis accompanying a spontaneous replication of molecules. It contains an additive noise term (Gaussian white noise) and a multiplicative noisy driving (dichotomous noise) in the term responsible for inhibition of population growth. This model may be used e.g. to describe an effect of cell-mediated immune surveillance against cancer. Specifically the relative rate of neoplastic cell destruction is a random dichotomous process due to the action of cytokines on the immune system.

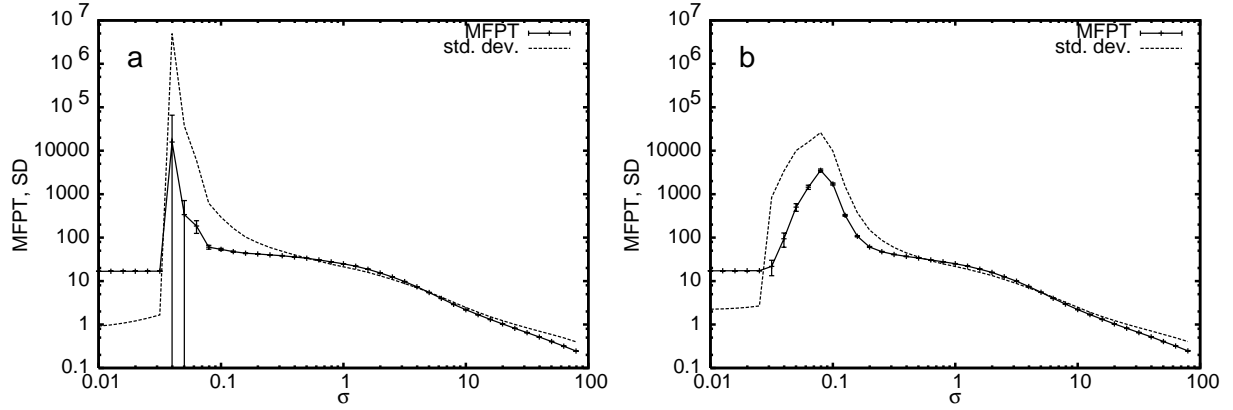


FIG. 8: MFPT and its standard deviation, with error bars, as a function of the additive noise intensity  $\sigma$  for two values of the correlation time  $\tau$ , namely (a)  $\tau = 1$  and (b)  $\tau = 10^5$ . Number of simulation runs  $N = 10^4$ , initial position of the Brownian particle  $x_{in} = 3.6$ . All the other parameter values are the same as in Fig. 2. The asymmetry of appearance of error bars near the maximum in Fig. 8a is due to the large values of error bar in these points and to the log scale.

We examined how the two different sources of noise influence the population's extinction time, identified with the mean first passage time of the system over the zero population state.

The first result obtained concerns the confirmation of the existence of noise enhanced stability (NES) phenomenon in a system in the absence of multiplicative noise as well as in its presence. The NES effect increases the extinction time as a function of the intensity of additive noise. The second result we have found in our study is the presence of resonant activation (RA) effect. This phenomenon minimizes the extinction time as a function of the correlation time of multiplicative noise. The two effects are acting in an opposite way in the cancer growth dynamics. Namely, the NES effect by increasing the lifetime of the metastable state delays the escape from the tumor state, while the RA effect by decreasing this lifetime leads to the extinction of the tumor. An appropriate choice of values of the noise parameters allows either to maximize or minimize the extinction time of the population.

Another result is the evidence for the possibility of co-occurrence of both mentioned noise-induced effects: resonant activation can be observed also in the region of noise-enhanced stability. In this coexistence region the NES effect which enhances the stability of tumoral state becomes strongly reduced by the RA mechanism which enhances the cancer extinction. In other words, an asymptotic regression to the zero tumor size may be induced by controlling the noise affecting hyperbolic inhibition of a spontaneous proliferation of cells.

An important part of this work is the analysis of the variance of first passage times compared to its mean, as the function of the noise intensity. This allowed us to fully explain the mechanisms underlying the resonant phenomena observed: the Arrhenius diffusive behavior in the range of high intensities of the additive noise; the divergence from the latter due to "trapping" events in the intermediate region where noise-enhanced stability occurs; and, finally, the domination of deterministic kinetics, with contributions from the stochastic diffusion visible mostly in a flat part of the potential well.

Our simple theoretical model can help to obtain new insight into the complexity of tumor progression, and at the same time may lead to new experiments in which the modulating activity

of cytokines can be driven by chemical agents or light irradiation. Of course there are many other factors characterizing the dynamics of the cancer growth due to the complexity of the system and due to many different types of cancer diseases.

### **Acknowledgments**

This work was supported by the ESF funds (via the STOCHDYN program) and MIUR. Additionally, A.O-M and E.G-N acknowledge financial support from the Polish State Committee for Scientific Research through the grants 1P03B15929 (2005-2007) and 2P03B08225.

We greatly thank Dr. C. Tripodo, of the Inst. of Anatomy and Pathological Histology of Palermo University, and Dr. A. Sica, of the Inst. of Pharmacological Researches M. Negri (Milano), for useful and deep discussions on the medical aspects of the cancer growth dynamics.



- 
- [1] W. Horsthemke, R. Lefever, *Noise-Induced Transitions. Theory and Applications in Physics, Chemistry and Biology*, (Springer-Verlag, Berlin, 1984).
  - [2] L. Gammaitoni *et al.*, Rev. Mod. Phys. **70**, 223 (1998).
  - [3] V.S. Anishchenko *et al.*, *Nonlinear dynamics of chaotic and stochastic systems*, (Springer Verlag, 2003).
  - [4] J. Tyson, B. Novak, J. Theor. Biol. **210**, 249 (2001); J.J. Tyson, K.C. Chen, B. Novak, Curr. Opin. Cell Biol **15**, 221 (2003); M. Tomita *et al.*, Bioinformatics **15**, 72 (1999).
  - [5] F.A. Cucinotta and J.F. Dicello, Adv. Space Res. **25**, 2131 (2000).
  - [6] J. Kiefer, *A repair fixation model based on classical enzyme kinetics* In J. Kiefer (ed), Quantitative Models in Radiation Biology (Springer Verlag, Berlin, 1988); R.K. Sachs, P. Hahnfeld and D.J. Brenner, Int. J. Radiat. Biol. **72**, 351 (1997).
  - [7] F. Messier, Ecology **75** (2), 478 (1994); J.M. Fryxell *et al.*, Ecology **80** (4), 1311 (1999).
  - [8] E. Sala, M.H. Graham, Proc. Natl. Acad. Sci. USA **99** (6), 3678 (2002); J.M. Levine, C.M. D'Antonio, Conservation Biology **17** (1), 322 (2003); S. K. Banik, *Correlated noise induced control of prey extinction*, (arXiv:physics/01100088) (2001).
  - [9] I. Prigogine, R. Lefever, Comp. Biochem. Physiol. **67B**, 389 (1980).
  - [10] P. Zhivkov, J. Waniewski, Int. J. Appl. Math. Comput. Sci. **13** (3), 307 (2003).
  - [11] R. Lefever, W. Horsthemke, Bull. of Math. Biol **41**, 469 (1979).
  - [12] R.P. Garay and R. Lefever, J. Theor. Biol. **73**, 417 (1978).
  - [13] N.S. Goel, N. Richter-Dyn, *Stochastic models in biology* (Academic Press, 1974).
  - [14] A. Mantovani, A. Sica, *et al.*, Trends Immunol. **25**, 677 (2004).
  - [15] A. Mantovani, P. Allavena, A. Sica, Eur. J. Cancer **40**, 1660 (2004).
  - [16] R. L. Elliott and G. C. Blobe, J. Clin. Oncol. **23**, 2078 (2005).
  - [17] A. Ochab-Marcinek and E. Gudowska-Nowak, Physica A **343**, 557 (2004).
  - [18] T. G. Kurtz, *Approximation of Population Processes*, (SIAM, Philadelphia, 1981); C.W. Gardiner, *Handbook of stochastic methods*, (Springer Verlag, Berlin, 1985).
  - [19] P. Hänggi, H. Grabert, P. Talkner, H. Thomas, Phys. Rev A **29**, 371 (1984).
  - [20] M. Samoilov, S. Plyasunov, A. P. Arkin, Proc. Natl. Acad. Sci. USA **102**, 2310 (2005); C. V. Rao and A. P. Arkin, J. Chem. Phys. **118**, 4999 (2003); M. R. Roussel and R. Zhu, *ibidem* **121**, 8716 (2004); M. Frankowicz *et al.*, J. Phys. Chem. **97**, 1891 (1993).
  - [21] For example, interleukin-2 activates a cell-mediated immune response, while interleukin-4 and interleukin-10 suppress cell-mediated responses.
  - [22] C. R. Doering and J. C. Gadoua, Phys. Rev. Lett. **69**, 2318 (1992).
  - [23] M. Bier and R. D. Astumian, Phys. Rev. Lett. **71**, 1649 (1993); P. Pechukas and P. Hänggi, *ibidem* **73**, 2772 (1994); P. Reimann, *ibidem* **74**, 4576 (1995).
  - [24] J. Iwaniszewski, Phys. Rev. E **54**, 3173 (1996).
  - [25] M. Boguñá, J. M. Porra, J. Masoliver, and K. Lindenberg, Phys. Rev. E **57**, 3990 (1998).
  - [26] P. Reimann, R. Bartussek and P. Hänggi, Chem. Phys. **235**, 11 (1998).
  - [27] M. Bier, I. Derenyi, M. Kostur, D. Astumian, Phys. Rev. E **59**, 6422 (1999).
  - [28] R. N. Mantegna and B. Spagnolo, Phys. Rev. Lett. **84**, 3025 (2000); J. Phys. IV (France) **8**, 247 (1998).
  - [29] B. Dybiec, E. Gudowska-Nowak, Phys. Rev. E **66**, 026123 (2002).
  - [30] R. N. Mantegna and B. Spagnolo, Phys. Rev. Lett. **76**, 563 (1996).
  - [31] N. V. Agudov and B. Spagnolo, Phys. Rev. E **64**, 035102(R) (2001).

- [32] A. A. Dubkov, N. V. Agudov, and B. Spagnolo, Phys. Rev. E **69**, 0161103 (2004).
- [33] A. L. Pankratov and B. Spagnolo, Phys. Rev. Lett. **93**, 177001 (2004).
- [34] A. Fiasconaro, B. Spagnolo and S. Boccaletti, Phys. Rev. E **72**, 061110(5) (2005).
- [35] The correspondence with a thermal noise is a loose one, since a process of the population growth and extinction goes on rather in a changing environment and the spontaneous fluctuations of the densities of cells do not follow the fluctuation-dissipation theorem.
- [36] Exponential distribution of first passage times describes the distance between events with uniform distribution in time. If  $t$  stands for time variable and  $\lambda t$  is the expected number of events in the interval  $[0, t]$  then  $e^{-\lambda t}$  is the probability of no events in  $[0, t]$ . Consequently, for the exponential pdf  $\lambda e^{-\lambda t}$  the ratio between the first moment  $\langle t \rangle$  and the standard deviation  $\sqrt{Var[t]}$  is equal to 1.